Report

Cell Reports

The C-type Lectin Receptor CLEC12A Recognizes Plasmodial Hemozoin and Contributes to Cerebral Malaria Development

Graphical Abstract

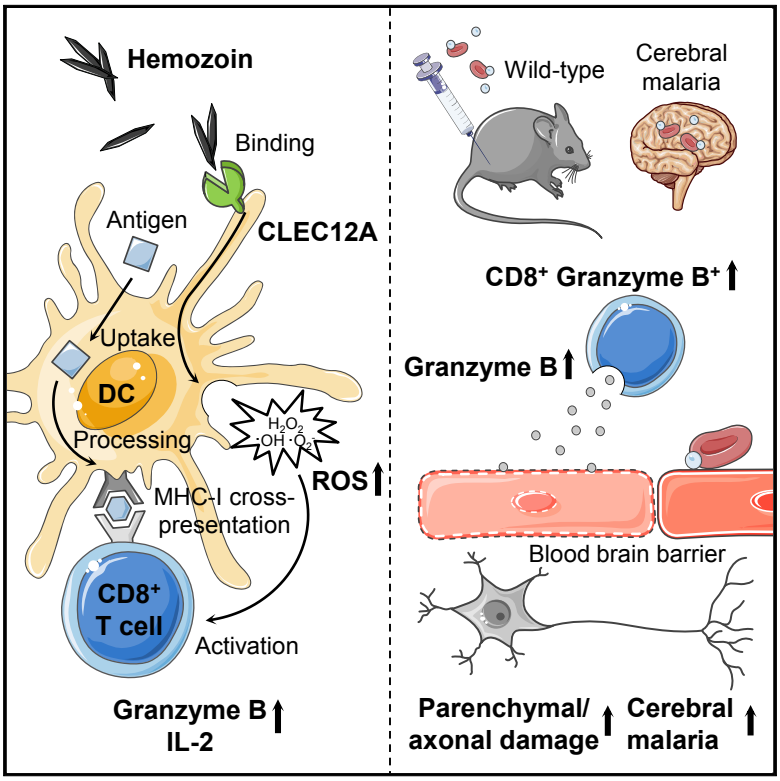

Authors

Marie-Kristin Raulf, Timo Johannssen, Svea Matthiesen, ..., Christina Strube, Jürgen Ruland, Bernd Lepenies

Correspondence

bernd.lepenies@tiho-hannover.de

In Brief

Raulf et al. demonstrate that CLEC12A recognizes plasmodial hemozoin and is involved in the development of experimental cerebral malaria (ECM). *In vivo* studies show a reduction in ECM in CLEC12A$^{-/-}$ mice that is accompanied by a decrease in the frequency of brain-sequestered granzyme B-expressing T cells.

Highlights

- CLEC12A recognizes plasmodial hemozoin
- The CLEC12A/hemozoin interaction enhances CD8^{+} T cell cross-priming *in vitro*
- CLEC12A$^{-/-}$ mice are protected from experimental cerebral malaria

Raulf et al., 2019, Cell Reports *28*, 30–38
July 2, 2019
https://doi.org/10.1016/j.celrep.2019.06.015

CellPress

OPEN ACCESS
CellPress

Cell Reports
Report

The C-type Lectin Receptor CLEC12A Recognizes Plasmodial Hemozoin and Contributes to Cerebral Malaria Development

Marie-Kristin Raulf,[1,2,12] Timo Johannssen,[1,3,4,12] Svea Matthiesen,[1] Konstantin Neumann,[5,6] Severin Hachenberg,[1] Sabine Mayer-Lambertz,[1] Fridolin Steinbeis,[3,7] Jan Hegermann,[8] Peter H. Seeberger,[3,4] Wolfgang Baumgärtner,[9] Christina Strube,[2] Jürgen Ruland,[5,10,11] and Bernd Lepenies[1,3,4,13,*]

[1]Immunology Unit and Research Center for Emerging Infections and Zoonoses, University of Veterinary Medicine Hannover, 30559 Hannover, Lower Saxony, Germany
[2]Institute for Parasitology, Centre for Infection Medicine, University of Veterinary Medicine Hannover, 30559 Hannover, Lower Saxony, Germany
[3]Department of Biomolecular Systems, Max Planck Institute of Colloids and Interfaces, 14476 Potsdam, Brandenburg, Germany
[4]Department of Biology, Chemistry and Pharmacy, Institute of Chemistry and Biochemistry, Freie Universität Berlin, 14195 Berlin, Germany
[5]Institut für Klinische Chemie und Pathobiochemie, Klinikum rechts der Isar, Technische Universität München, 81675 Munich, Bavaria, Germany
[6]Institute of Clinical Chemistry, Hannover Medical School, 30625 Hannover, Lower Saxony, Germany
[7]Charité-Universitätsmedizin Berlin, Klinik mit Schwerpunkt Infektiologie und Pneumologie, 13353 Berlin, Berlin, Germany
[8]Research Core Unit Electron Microscopy, Hannover Medical School, 30625 Hannover, Lower Saxony, Germany
[9]Department of Pathology, University of Veterinary Medicine Hannover, 30559 Hannover, Lower Saxony, Germany
[10]German Cancer Consortium (DKTK), 69120 Heidelberg, Baden-Württemberg, Germany
[11]German Center for Infection Research (DZIF), Partner Site Munich, Munich, Bavaria, Germany
[12]These authors contributed equally
[13]Lead Contact
*Correspondence: bernd.lepenies@tiho-hannover.de
https://doi.org/10.1016/j.celrep.2019.06.015

SUMMARY

Malaria represents a major cause of death from infectious disease. Hemozoin is a *Plasmodium*-derived product that contributes to progression of cerebral malaria. However, there is a gap of knowledge regarding how hemozoin is recognized by innate immunity. Myeloid C-type lectin receptors (CLRs) encompass a family of carbohydrate-binding receptors that act as pattern recognition receptors in innate immunity. In the present study, we identify the CLR CLEC12A as a receptor for hemozoin. Dendritic cell-T cell co-culture assays indicate that the CLEC12A/hemozoin interaction enhances $CD8^+$ T cell cross-priming. Using the *Plasmodium berghei* Antwerpen-Kasapa (ANKA) mouse model of experimental cerebral malaria (ECM), we find that CLEC12A deficiency protects mice from ECM, illustrated by reduced ECM incidence and ameliorated clinical symptoms. In conclusion, we identify CLEC12A as an innate sensor of plasmodial hemozoin.

INTRODUCTION

Malaria represents a major cause of death from infectious disease, resulting in 216 million new cases and an estimated 445,000 deaths in 2016 (WHO, 2017). The disease is caused by infection with obligate intraerythrocytic apicomplexan parasites of the genus *Plasmodium*. *P. falciparum* represents a major morbidity factor due to the development of severe malaria; e.g., cerebral malaria (Newton et al., 1998). Infection of susceptible mice with *Plasmodium berghei* Antwerpen-Kasapa (ANKA) (PbA) is a commonly accepted model for *Plasmodium*-induced inflammation. Experimental cerebral malaria (ECM) pathology induced by PbA infection encompasses neurovascular inflammation with neurological symptoms such as cognitive dysfunction, ataxia, paralysis, convulsions, and coma, ultimately leading to death (de Oca et al., 2013).

Immunopathology during PbA infection has been extensively studied. ECM is predominantly mediated by brain-sequestered T cells (Boubou et al., 1999; Grau et al., 1986; Hermsen et al., 1997, 1998; Yañez et al., 1996). $CD8^+$ T cells in particular are crucial for ECM pathogenesis by release of perforin and granzyme B (GrB), promoting tissue damage and compromising blood-brain barrier integrity (Haque et al., 2011; Nitcheu et al., 2003; Potter et al., 2006). Naive T cells are primed by conventional $CD11c^+$ dendritic cells (DCs) in the spleen (cross)presenting PbA-derived antigens; thus, DCs contribute to T cell-mediated pathology during malaria (deWalick et al., 2007).

Besides brain-sequestered T cells, a pro-inflammatory cytokine milieu is linked to the disease that is believed to be provoked by *Plasmodium*-derived hemozoin. Hemozoin crystals constitute a disposal product generated during intra-erythrocytic parasite development. After infection of red blood cells (RBCs), the parasite consumes up to 80% of the hemoglobin and crystallizes otherwise toxic heme monomers into insoluble hemozoin (Coronado et al., 2014). Hemozoin crystals are released during host cell rupture and rapidly ingested by phagocytes with subsequent

production of pro-inflammatory cytokines, nitric oxide (NO), and reactive oxygen species (ROS) at the early onset of disease (Olivier et al., 2014; Shio et al., 2010; Tyberghein et al., 2014). For instance, hemozoin is known to induce activation of the NLRP3/inflammasome complex via potassium efflux, phagocytosis, and ROS production, leading to release of the pro-inflammatory cytokine interleukin-1β (IL-1β) (Dostert et al., 2009; Shio et al., 2009). Fatal malaria cases are characterized by increased numbers of monocytes and neutrophils carrying intracellular hemozoin deposits (Nguyen et al., 1995). ECM-susceptible mice infected with PbA exhibit significantly increased levels of hemozoin in the brain, in contrast to mice infected with the non-ECM-inducing *P. berghei* strain NK65 (Sullivan et al., 1996). Hence, although hemozoin has been shown to be immunologically active *in vitro* and *in vivo*, the cellular receptors recognizing hemozoin remain elusive.

It has been shown that pattern recognition receptors (PRRs) such as Nod-like receptors (NLRs) are important mediators of ECM pathogenesis *in vivo* (Dostert et al., 2009), whereas the role of Toll-like receptors (TLRs) in ECM development is debated (Coban et al., 2007; Lepenies et al., 2008; Togbe et al., 2007). TLR2 and TLR4 recognize *P. falciparum* glycosylphosphatidyl inositol (GPI) anchors, thus mediating cytokine and NO production (Krishnegowda et al., 2005). Additionally, TLR9 senses CpG and adenine thymine (AT) motifs in plasmodial DNA present on the surface of *Plasmodium*-derived hemozoin (Parroche et al., 2007). In contrast, there is a gap of knowledge regarding the contribution of C-type lectin receptors (CLRs) to immunity during the course of malaria. The F-Actin-recognizing CLR CLEC9A defines a DC subset that is crucial for ECM development via cross-priming of $CD8^+$ T cells (Piva et al., 2012). We have shown previously that the DC immunoreceptor (DCIR) markedly alters the course of disease since $DCIR^{-/-}$ mice are significantly protected from ECM (Maglinao et al., 2013). However, direct recognition of a *Plasmodium*-derived ligand by CLRs has so far not been shown.

The myeloid inhibitory C-type lectin-like receptor (CLEC12A) is a type II transmembrane protein predominantly expressed by innate immune cells such as granulocytes, macrophages, and DCs (Lahoud et al., 2009; Pyz et al., 2008). CLEC12A can be exploited to deliver tumor antigens into DCs, inducing efficient activation of $CD8^+$ T cells by cross-priming (Hutten et al., 2016), and can be efficiently targeted to induce influenza antigen-specific tissue-resident memory $CD8^+$ T cells (Wakim et al., 2015). A recent study identified monosodium urate (MSU) crystals as a CLEC12A ligand, highlighting an important role of CLEC12A in recognition of dead cells. In this context, CLEC12A is critically involved in the MSU-mediated respiratory burst by interfering with Syk signaling (Neumann et al., 2014).

To identify *Plasmodium*-derived CLR ligands, we employed a CLR-human Fc (hFc) fusion protein library (Maglinao et al., 2014; Monteiro et al., 2019) and observed strong binding of CLEC12A-hFc to parasitized RBC (pRBC)-derived lysates and permeabilized pRBCs. Reporter cell assays, flow cytometry-based assays, and fluorescence microscopy revealed hemozoin crystals as a CLEC12A ligand. Hemozoin affected ROS production by bone marrow-derived DCs (BMDCs) and ovalbumin $(OVA)_{257–264}$ peptide cross-presentation by BMDCs to OT-I T cell receptor (TCR)-transgenic T cells in a CLEC12A-dependent fashion. *In vivo* challenge of $CLEC12A^{-/-}$ mice with PbA resulted in reduced ECM incidence and attenuated ECM symptoms, accompanied by reduced expression of granzyme B in T cells derived from brains and spleens of infected mice. Taken together, this study provides a mechanism by which hemozoin is recognized by innate immunity and reveals an important role of CLEC12A in immunopathology during malaria.

RESULTS

CLEC12A Recognizes Hemozoin

We demonstrated previously that DCIR plays a crucial role in ECM development (Maglinao et al., 2013). However, DCIR does not bind to parasite-derived ligands but, rather, recognizes endogenous damage-associated molecular patterns (DAMPs; Bloem et al., 2014). Thus, to identify CLR interactions with *Plasmodium*-derived ligands, we employed a CLR-hFc fusion protein library (Maglinao et al., 2014; Monteiro et al., 2019). Initial screenings were carried out using *P. falciparum*-infected RBCs. We observed marked binding for CLEC12A-hFc as opposed to the hFc control or other CLR-hFc chimeras, such as DCIR-hFc, DC immunoactivating receptor (DCAR)-hFc, macrophage C-type lectin (MCL)-hFc, and CLEC9A-hFc (Figure 1A). Binding was confirmed using PbA pRBCs (Figure 1B), indicating that CLEC12A recognizes a plasmodial component present in different *Plasmodium* species. To identify whether CLEC12A recognizes an intracellular component within *Plasmodium*-infected RBCs, we analyzed binding to pRBCs by fluorescence microscopy upon RBC permeabilization. Indeed, CLEC12A-hFc specifically bound to permeabilized pRBCs, suggesting that CLEC12A recognizes an internal ligand present in pRBCs (Figure 1C).

Because CLEC12A was recently shown to bind to uric acid crystals (Neumann et al., 2014), we hypothesized that this CLR might be involved in the recognition of hemozoin crystals. Although many protocols for the synthesis of hemozoin yield material that is poorly crystalline (Jaramillo et al., 2009), we used synthetic hemozoin that resembled natural hemozoin in size (0.5–1 μm), as confirmed by electron microscopy (Figure S1A). Indeed, both human CLEC12A-hFc as well as murine CLEC12A-hFc bound to synthetic hemozoin, as demonstrated by flow cytometry (Figure 1D) and fluorescence microscopy (Figure 1E). To analyze whether hemozoin acts as an agonistic ligand of CLEC12A, reporter cell assays were performed. Because binding of MSU to the CLEC12A reporter cell line has been demonstrated previously (Neumann et al., 2014), MSU was used as a positive control. Hemozoin showed marked activation of cells expressing human CLEC12A and, to a lower extent, murine CLEC12A (Figure 1F). Even lysates of *Plasmodium*-infected RBCs induced activation of CLEC12A reporter cells compared with uninfected RBCs, indicating that hemozoin can be recognized by CLEC12A at physiological concentrations (Figure S1B). These findings clearly show that hemozoin acts as an agonistic ligand of the CLR CLEC12A.

CLEC12A Impairs DC Effector Functions *In Vitro*

CLEC12A is mainly expressed by DCs (Lahoud et al., 2009). Therefore, we assessed the effect of the hemozoin/CLEC12A

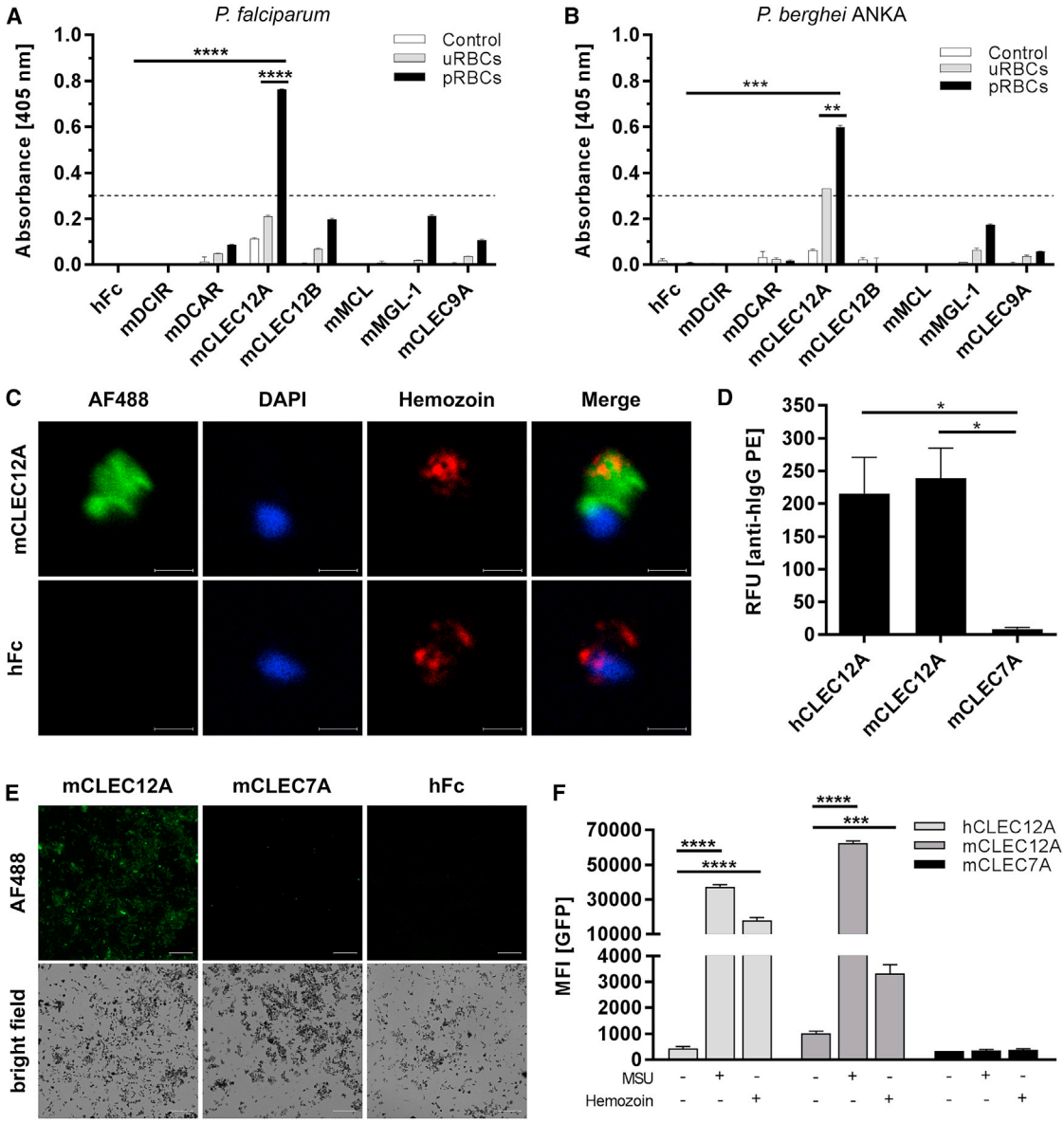

Figure 1. CLEC12A Recognizes Hemozoin

(A and B) ELISA-based binding studies with (A) *P. falciparum* and (B) *P. berghei* ANKA. Isolated parasitized RBCs (pRBCs) were lysed, immobilized on microtiter plates, and probed with the indicated fusion proteins. Lysates from uninfected RBCs (uRBCs) and PBS alone (control) were used as controls. Data are presented as mean + SEM and representative of three independent experiments in duplicates for *P. falciparum* (n = 3) and two experiments in duplicates for *P. berghei* ANKA (n = 2).

(C) Fluorescence microscopy of permeabilized pRBCs. Permeabilized pRBCs were incubated with CLEC12A-hFc, followed by staining with an anti-human immunoglobulin G (IgG) (Fc) Alexa Fluor 488-labeled antibody (AF488, green). Parasitic DNA was stained with DAPI (blue). Hemozoin fluorescence was visualized using a 633-nm HeNe laser (hemozoin, red). pRBCs probed with hFc served as a negative control. Data are representative of two independent experiments (n = 2). Scale bars represent 1 μm.

(D) Flow cytometry-based binding studies with hemozoin. Hemozoin was probed with the indicated fusion proteins. CLEC7A-hFc served as a negative control. Means + SD of three independent experiments (n = 3) are shown.

(E) Fluorescence microscopy of synthetic hemozoin. Hemozoin was probed with the indicated hFc fusion proteins and incubated with an anti-human IgG (Fc) Alexa Fluor 488 antibody (AF488, green). Samples incubated with hFc served as a negative control. Data are representative of two independent experiments (n = 2). Scale bars represent 10 μm.

(F) Recognition of hemozoin (100 μg/mL) and MSU (250 μg/mL) by human (h) and murine (m) CLEC12A-CD3 reporter cell lines. A murine CLEC7A-CD3 reporter cell line served as a negative control. Data are presented as mean + SD and are representative of three independent experiments (n = 3) in triplicates (two experiments) or quadruplicates (one experiment).

Statistical significance was evaluated using unpaired (ELISA, reporter cell assay) or paired (flow cytometry-based binding studies) two-tailed Student's t test. Asterisks indicate significant differences (*p < 0.05, **p < 0.01, ***p < 0.001, ****p < 0.0001). See also Figure S1.

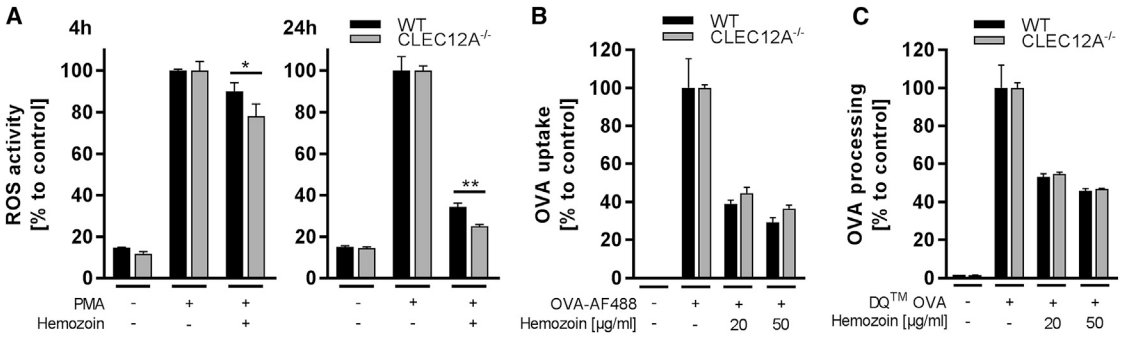

Figure 2. Hemozoin Recognition by CLEC12A Affects DC Effector Functions

(A) CLEC12A$^{-/-}$ or wild-type (WT) bone marrow-derived dendritic cells (BMDCs) were treated with hemozoin (100 μg/mL) for 4 h or 24 h, respectively. After hemozoin stimulation, ROS production was induced by stimulation with PMA (100 ng/mL) and evaluated using DHR-123.

(B and C) CLEC12A$^{-/-}$ or WT BMDCs were pulsed with (B) Alexa Fluor 488-labeled ovalbumin (OVA-AF488) (25 μg/mL) to assess antigen uptake or (C) DQ OVA (25 μg/mL) to measure antigen processing.

All data are representative of three experiments (n = 3) in triplicates, displayed as mean + SD and expressed as percentages to control after normalization to the mean fluorescence intensities of the respective samples stimulated with PMA or OVA only. Statistical analysis was performed using unpaired two-tailed Student's t test. Asterisks indicate significant differences (*$p < 0.05$, **$p < 0.01$). See also Figure S2.

interaction on DC effector functions by stimulating BMDCs from CLEC12A$^{-/-}$ and wild-type (WT) mice with hemozoin. Hemozoin is known to interfere with ROS production of antigen-presenting cells (APCs), depending on the stimulation conditions (Cambos et al., 2010; Schwarzer and Arese, 1996; Shio et al., 2010). Hence, BMDCs were stimulated with hemozoin for 4 h or 24 h, followed by ROS induction using phorbol 12-myristate-13-acetate (PMA). Hemozoin slightly reduced the capacity to produce ROS after 4 h and strongly after 24 h incubation in both WT and CLEC12A$^{-/-}$ BMDCs. Strikingly, reduction of ROS production was more pronounced in CLEC12A$^{-/-}$ BMDCs (ROS activity after 4 h: WT 90.2%, CLEC12A$^{-/-}$ 78.1%; ROS activity after 24 h: WT 34.4%, CLEC12A$^{-/-}$ 25.0%), indicating that hemozoin-impaired ROS production is at least partially CLEC12A dependent (Figure 2A). Interestingly, we did not observe differences in overall hemozoin internalization by DCs, indicating that CLEC12A did not act as a phagocytic receptor (data not shown). To assess whether the CLEC12A/hemozoin interaction had an effect on antigen uptake and processing, BMDCs were stimulated with Alexa Fluor 488-labeled OVA (to assess antigen uptake) or DQ OVA (to measure antigen processing) in the presence or absence of hemozoin. OVA uptake and processing were not impaired by the CLEC12A/hemozoin interaction (Figures 2B and 2C). Additional DC effector functions were monitored by stimulating BMDCs in the presence or absence of hemozoin. However, no differences were observed in pro-inflammatory cytokine secretion (Figure S2A) or expression of activation markers (Figure S2B) between WT and CLEC12A$^{-/-}$ BMDCs. These findings indicate that the CLEC12A/hemozoin interaction selectively affected ROS production by BMDCs.

CLEC12A Affects T Cell Activation *In Vitro*

To unravel the CLEC12A/hemozoin interaction on DCs and subsequent T cell priming mechanistically, antigen presentation assays using BMDCs from CLEC12A$^{-/-}$ mice and WT control mice were conducted. Because CD8$^+$ T cells play a pivotal role in ECM induction, the CD8$^+$ T cell response to cross-presented OVA$_{257–264}$ peptide was measured using OT-I TCR-transgenic CD8$^+$ T cells. To this end, cytokine release by OT-I CD8$^+$ T cells was measured by ELISA, and intracellular cytokine accumulation was determined by flow cytometry (see Figure S3A for gating of cells). Upon OVA stimulation alone, cytokine secretion and frequency of cytokine-producing T cells were slightly higher when T cells were co-cultured with CLEC12A$^{-/-}$ BMDCs, consistent with the putative role of CLEC12A as an inhibitory receptor. Thus, to exclude intrinsic hemozoin-independent effects, data were normalized to stimulation with OVA only. Hemozoin enhanced CD8$^+$ T cell responses, as indicated by increased production of GrB, IL-2, tumor necrosis factor alpha (TNF-α), and interferon γ (IFN-γ) as well as an elevated number of cytokine-positive T cells (Figures 3A and S3B). However, hemozoin-enhanced IL-2 production was completely abolished, GrB production reduced, and TNF-α production slightly reduced when CLEC12A$^{-/-}$ BMDCs were used to stimulate OT-I T cells. Similar effects were observed for the number of cytokine-expressing T cells (Figure S3B). These findings highlight involvement of CLEC12A in cross-presentation of antigens. A similar effect was found for expression of the T cell activation marker CD69 (Figure S3C). In contrast, only minor effects of the CLEC12A/hemozoin interaction on cytokine production by OT-II TCR-transgenic CD4$^+$ T cells (activated by the OVA$_{323–339}$ peptide) were observed (Figure 3B). Taken together, DC-T cell co-cultures show that the stimulatory effect of the CLEC12A/hemozoin interaction is mainly restricted to cross-priming of CD8$^+$ T cells.

CLEC12A Contributes to ECM Development and Affects Granzyme B Expression by T Cells

The marked effect of the CLEC12A/hemozoin interaction on CD8$^+$ T cell priming *in vitro* prompted us to evaluate the role of CLEC12A *in vivo*. Therefore, we challenged CLEC12A$^{-/-}$ mice with PbA and assessed ECM pathogenesis. As expected, WT mice displayed neurological symptoms within 7–10 days post

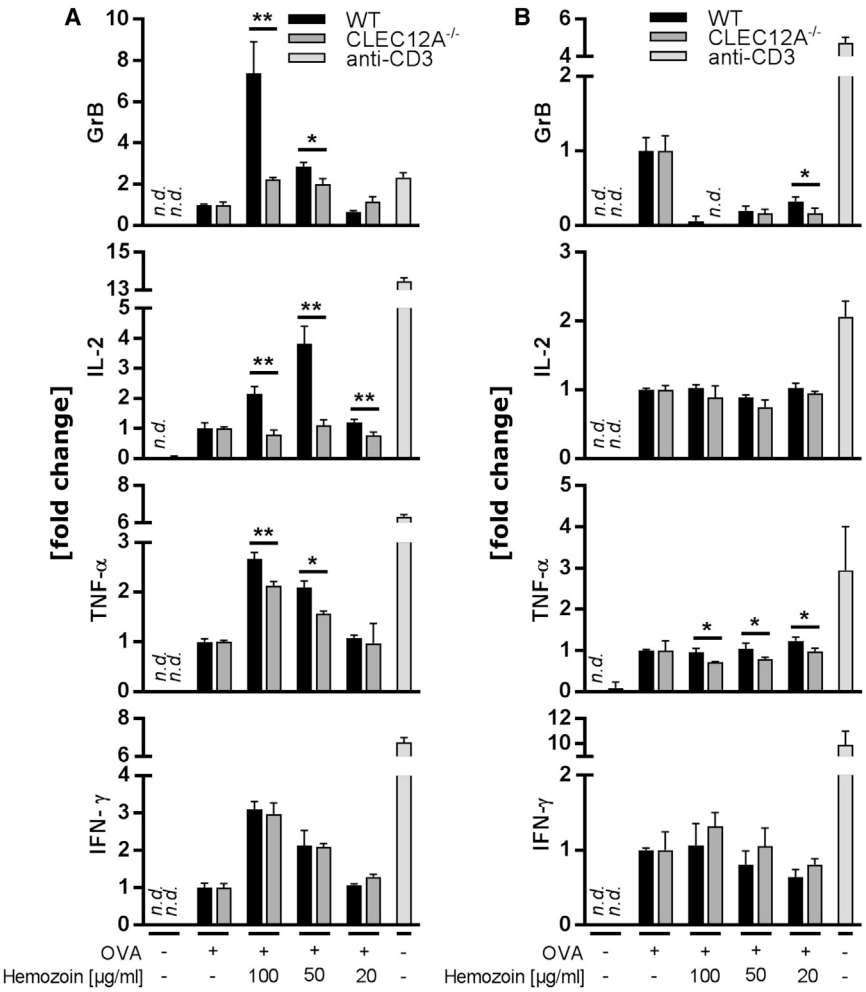

Figure 3. Hemozoin Recognition by CLEC12A Affects CD8$^+$ T Cell Priming

CLEC12A$^{-/-}$ or WT BMDCs were pulsed with EndoGrade OVA (300 μg/mL) in the presence or absence of hemozoin. BMDCs were co-cultured with either OT-I or OT-II receptor transgenic T cells. Anti-CD3 (5 μg/mL)-stimulated T cells served as a positive control.

(A) OT-I CD8$^+$ T cell secretion of granzyme B (GrB), IL-2, TNF-α, and IFN-γ. Mean cytokine production of samples stimulated with OVA only ranged from 1,470 pg/mL (WT) to 2,308 pg/mL (CLEC12A$^{-/-}$) for GrB, 106 pg/mL (WT) to 133 pg/mL (CLEC12A$^{-/-}$) for IL-2, 104 pg/mL (WT) to 119 pg/mL (CLEC12A$^{-/-}$) for TNF-α, and 1,022 pg/mL (WT) to 866 pg/mL (CLEC12A$^{-/-}$) for IFN-γ.

(B) OT-II CD4$^+$ T cell secretion of GrB, IL-2, TNF-α, and IFN-γ. Mean cytokine production of samples stimulated with OVA only ranged from 502 pg/mL (WT) to 448 pg/mL (CLEC12A$^{-/-}$) for GrB, 427 pg/mL (WT) to 490 pg/mL (CLEC12A$^{-/-}$) for IL-2, 88 pg/mL (WT) to 100 pg/mL (CLEC12A$^{-/-}$) for TNF-α, and 465 pg/mL (WT) to 342 pg/mL (CLEC12A$^{-/-}$) for IFN-γ.

Graphs are representatives of two (OT-I, n = 2) and three (OT-II, n = 3) independent experiments in triplicates. All data were normalized to the respective OVA stimulation, expressed as fold change and displayed as mean + SD. Statistical significance was evaluated using unpaired two-tailed Student's t test. Asterisks indicate significant differences (*p < 0.05, **p < 0.01). n.d., not detectable. See also Figure S3.

infection (p.i.) with a total ECM incidence of around 90%. Strikingly, CLEC12A$^{-/-}$ mice were significantly protected from ECM, enhancing the final survival rate after 14 days by 42% compared with WT mice (52% versus 10%; Figure 4A). Consistent with these findings, CLEC12A$^{-/-}$ mice showed a significantly reduced disease score over time (Figure 4B). No significant differences were observed regarding parasitemia levels between CLEC12A$^{-/-}$ and WT control mice, suggesting that CLEC12A deficiency does not affect parasite replication directly (Figure S4A).

To analyze systemic inflammation, pro-inflammatory serum cytokines were measured in PbA-infected CLEC12A$^{-/-}$ and WT mice. Overall, PbA infection enhanced the levels of TNF-α, IFN-γ, and IL-6. However, systemic inflammation was not altered in CLEC12A$^{-/-}$ mice compared with WT mice (Figure S4B). Quantitative T cell sequestration to the brain was not significantly altered in CLEC12A$^{-/-}$ mice despite a tendency toward reduced T cell numbers in the brain of CLEC12A$^{-/-}$ mice (Figure S4C). However, effector functions were markedly modulated in CLEC12A$^{-/-}$ mice, as indicated by a reduced frequency of brain-sequestered T cells expressing GrB (21.3% ± 3.9% versus 34.4% ± 6.1%; Figure 4C). Similar results were obtained for splenic T cells; frequencies of GrB$^+$ CD4$^+$ T cells (6.0% ± 1.1% versus 10.5% ± 1.2%) and CD8$^+$ T cells (13.9% ± 2.0% versus 22.1% ± 2.2%) were significantly reduced in CLEC12A$^{-/-}$ mice (Figure 4D).

In conclusion, these findings demonstrate that CLEC12A affects ECM development by enhancing T cell effector functions; namely, GrB expression by activated CD8$^+$ T cells.

DISCUSSION

Hemozoin constitutes a *Plasmodium*-derived disposal product involved in immunomodulation during malaria (Scorza et al., 1999). However, little is known about the cellular receptors recognizing hemozoin. It has been proposed that hemozoin is bound by TLR9 (Coban et al., 2005), likely by adsorbing *Plasmodium* DNA (Parroche et al., 2007), whereas the role of CLRs in hemozoin recognition has so far not been addressed. Recently, it has been reported that CLEC12A binds to uric acid crystals and subsequently regulates innate immune responses (Neumann et al., 2014). We thus hypothesized that the CLEC12A ligand present in *Plasmodium*-infected RBCs might be of crystalline origin. In this study, we identified

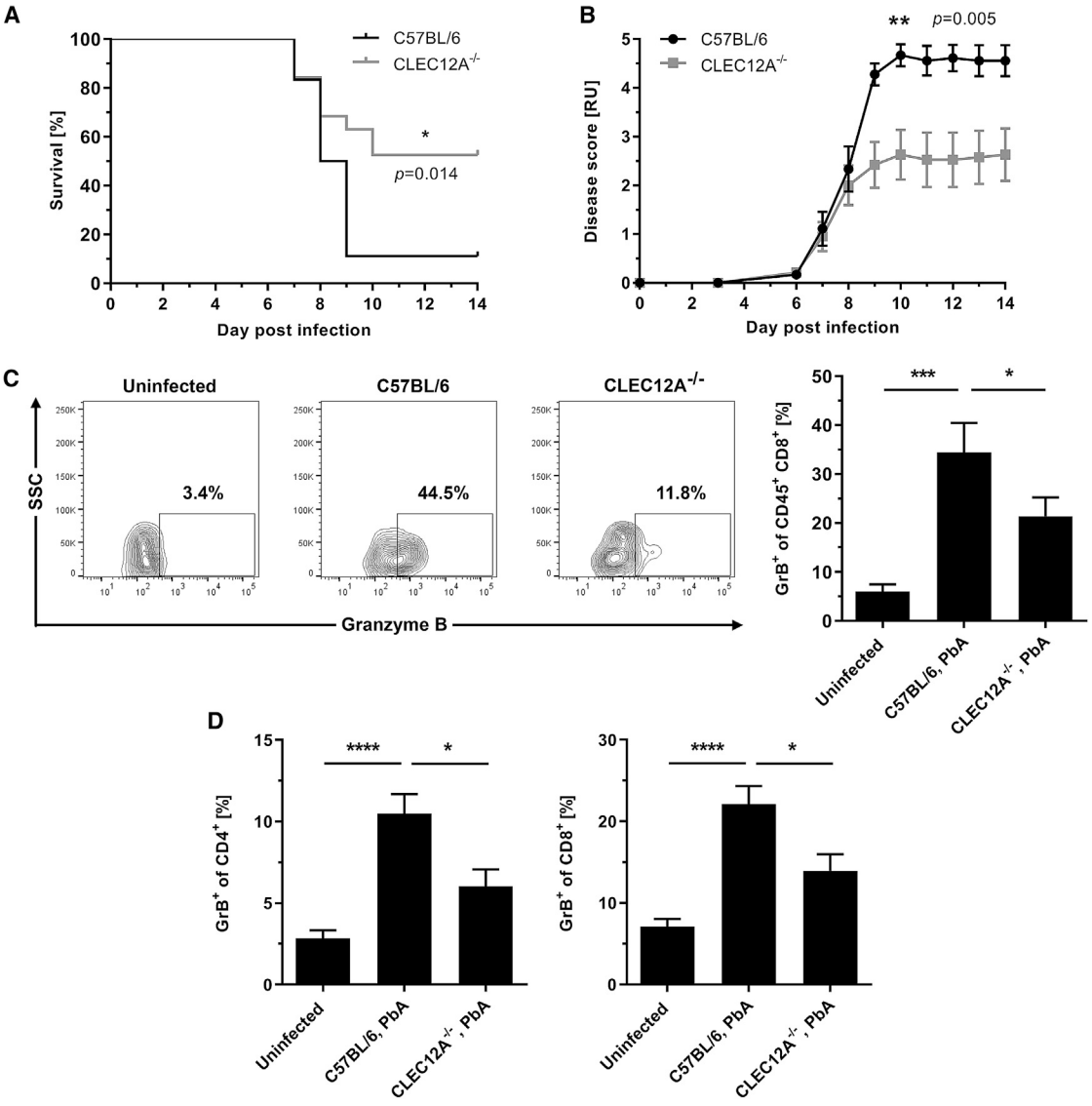

Figure 4. CLEC12A Deficiency Protects from ECM Development

(A and B) CLEC12A$^{-/-}$ and C57BL/6 control mice were challenged with PbA by intraperitoneal injection of 1 × 10^6 pRBCs and monitored for up to 14 days. The illustrated plots are summarized from three independent experiments (WT: n = 10, 4, 4; total n = 18 mice; CLEC12A$^{-/-}$: n = 9, 5, 5; total n = 19 mice). Statistical analysis was performed using log rank test (survival) or two-way repeated measures ANOVA (disease score).

(A) Survival of CLEC12A$^{-/-}$ mice compared with WT animals. Mice were euthanized at an early stage of ECM to minimize suffering (see STAR Methods for details).

(B) Disease score values reflecting the presence of symptoms. For each following day post sacrifice, a score of 5 was assigned. Data are expressed as mean ± SEM.

(C and D) PbA-infected CLEC12A$^{-/-}$ and C57BL/6 control mice were sacrificed on day 6 p.i., followed by flow cytometry measurement of GrB expression. Data are expressed as mean + SEM and summarized from two independent experiments (n = 3, 5; total n = 8 mice).

(C) Representative plots illustrating the frequency of GrB-expressing CD8$^+$ T cells in the brain with corresponding statistical analysis of GrB$^+$ CD8$^+$ T cells in the brain. Statistical analysis was performed using unpaired one-tailed Student's t test.

(D) Statistical analysis illustrating the frequency of splenic GrB-expressing CD4$^+$ and CD8$^+$ T cells. Statistical analysis was performed using unpaired two-tailed Student's t test.

Asterisks indicate significant differences (*p < 0.05, **p < 0.01, ***p < 0.001, ****p < 0.0001). See also Figure S4.

CLEC12A as a receptor for hemozoin using CLR-hFc fusion proteins and CLEC12A-CD3 reporter cells.

Because T cells, as an important cell subset mediating ECM, depend on activation by APCs, several studies addressed the role of DCs in ECM pathogenesis. It has been demonstrated that conventional DCs are of crucial importance for cross-priming of brain-sequestered CD8$^+$ T cells (deWalick et al., 2007; Lundie et al., 2008). However, it is largely unknown how DCs detect *Plasmodium* antigens and parasite-derived products. There is growing evidence that PRRs play distinct roles in ECM

pathogenesis *in vivo*, illustrated by previous findings regarding the effect of NLRs (Dostert et al., 2009) and TLRs (Coban et al., 2007; Lepenies et al., 2008; Togbe et al., 2007). In contrast, the role of CLRs in recognition of protozoan parasites has so far barely been addressed. In the present study, we observed a contribution of CLEC12A to hemozoin-dependent ROS production. Overall, PMA-induced ROS production by BMDCs was decreased upon hemozoin incubation, most prominently after 24 h. This is in agreement with previous findings where hemozoin has been reported to reduce ROS production in monocytes and macrophages, mainly after ingestion of the crystalline disposal product (Cambos et al., 2010; Schwarzer and Arese, 1996). Interestingly, ROS production was significantly reduced in CLEC12A$^{-/-}$ BMDCs compared with WT BMDCs, indicating that CLEC12A is involved in intracellular signaling leading to ROS production. Neumann et al. (2014) reported critical involvement of CLEC12A in MSU-mediated respiratory burst by interfering with Syk signaling. Furthermore, moderate levels of ROS are critical for efficient T cell activation and effector functions; for instance, IL-2 production (Franchina et al., 2018; Moro-García et al., 2018). In a recent study, ROS was shown to be involved in cross-presentation of antigens to CD8$^+$ T cells, where decreased ROS levels led to reduced CD8$^+$ T cell responses (Oberkampf et al., 2018). DC-T cell co-culture assays revealed a marked contribution of the hemozoin/CLEC12A interaction to CD8$^+$ T cell cross-priming. In particular, hemozoin-induced GrB and IL-2 production as well as the frequency of GrB$^+$ and IL-2$^+$ T cells were at least partly CLEC12A-dependent. IL-2 is known to positively regulate the expression of perforin and GrB in CD8$^+$ T cells (Janas et al., 2005; Tamang et al., 2006). Furthermore, the CLEC12A/hemozoin interaction partially abrogated TNF-α production and the frequency of TNF-α-positive T cells *in vitro*.

Infection of susceptible mouse lines with PbA is a commonly used model for *Plasmodium*-induced inflammation and underlines the importance of CD8$^+$ T cells for brain pathology via perforin- and GrB-dependent pathways (Haque et al., 2011; Nitcheu et al., 2003; Potter et al., 2006). To further investigate the role of the CLEC12A receptor in ECM pathology, CLEC12A$^{-/-}$ mice were infected with PbA. CLEC12A$^{-/-}$ mice displayed reduced ECM incidence and an ameliorated disease score, highlighting the crucial role of CLEC12A in PbA-mediated ECM development. However, this effect may not be exclusively mediated by the CLEC12A/hemozoin interaction. For instance, we cannot rule out that uric acid crystals or other endogenous CLEC12A ligands from damaged cells contribute to the *in vivo* effect of CLEC12A. Strikingly, GrB expression in brain-sequestered and splenic T cells was reduced in CLEC12A$^{-/-}$ mice during PbA infection. These findings suggest that CLEC12A does not markedly affect overall T cell activation and brain sequestration but, rather, modulates the quality of the T cell response by altering GrB expression levels. Targeting CLEC12A on DCs increased the frequency of GrB$^+$ T cells (Wakim et al., 2015). Interestingly, a recent study described a role of CLEC12A in induction of experimental autoimmune encephalomyelitis (EAE), where EAE disease induction was delayed and disease severity was reduced in CLEC12A$^{-/-}$ mice (Sagar et al., 2017).

Taken together, our study shows that CLEC12A recognizes *Plasmodium*-derived hemozoin. In addition, CLEC12A is critically involved in the development of ECM during PbA infection. The CLEC12A/hemozoin interaction affected ROS production by DCs and cross-presentation of plasmodial antigens to CD8$^+$ T cells. CLEC12A$^{-/-}$ mice exhibited significantly decreased ECM incidence during PbA infection, accompanied by a reduced frequency of GrB-expressing T cells in both the brain and spleen (Figure S4E). In summary, our findings demonstrate an important role of CLEC12A in hemozoin recognition and immune pathology during murine PbA infection. Future studies should further investigate the role of the CLEC12A/hemozoin interaction *in vivo*; for instance, by using other murine malaria models.

STAR★METHODS

Detailed methods are provided in the online version of this paper and include the following:

- KEY RESOURCES TABLE
- LEAD CONTACT AND MATERIALS AVAILABILITY
- EXPERIMENTAL MODEL AND SUBJECT DETAILS
  - Mouse model
  - Primary cell culture
- METHOD DETAILS
  - Culture of *Plasmodium* species
  - CLR-hFc binding assays
  - Fluorescence microscopy
  - Scanning electron microscopy
  - Reporter cell line assay
  - ROS assay
  - OVA uptake and processing
  - DC stimulation assay
  - DC-T cell co-culture assay
  - Challenge of mice with PbA
  - Flow cytometric analysis of T cells
- QUANTIFICATION AND STATISTICAL ANALYSIS

SUPPLEMENTAL INFORMATION

Supplemental Information can be found online at https://doi.org/10.1016/j.celrep.2019.06.015.

ACKNOWLEDGMENTS

B.L. acknowledges funding from the German Federal Ministry for Education and Research (BMBF; Fkz. 1615446), the DFG (SFB 765), and the Niedersachsen Research Network on Neuroinfectiology (N-RENNT-2). This work was also supported by research grants from the DFG (SFB 1054) and the ERC (FP7, grant agreement 322865) (to J.R.). P.H.S. gratefully acknowledges generous financial support from the Max Planck Society. We thank Susanne Eisenschmidt and Sandra Pfeifer for assistance with animal handling. Magdalena Eriksson, Maha Maglinao, Stephanie Zimmermann, Theresa Wagner, João Monteiro, and Silke Schöneberg helped with expression of CLR-hFc fusion proteins. Kerstin Rohn conducted electron microscopy. We are also grateful to Thomas Jacobs, who provided PbA stabilates.

AUTHOR CONTRIBUTIONS

T.J. and B.L. designed the research. M.-K.R., T.J., S.M., K.N., S.H., and F.S. performed the research. S.M.-L., J.H., P.H.S., W.B., C.S., and J.R. contributed

new reagents and/or analytical tools. M.-K.R., T.J., S.M., K.N., C.S., J.R., and B.L. analyzed data. M.-K.R., T.J., and B.L. wrote the paper with input from all other co-authors.

DECLARATION OF INTERESTS

The authors declare no competing interests.

Received: September 5, 2017
Revised: March 15, 2019
Accepted: June 4, 2019
Published: July 2, 2019

REFERENCES

Bloem, K., Vuist, I.M., van den Berk, M., Klaver, E.J., van Die, I., Knippels, L.M., Garssen, J., García-Vallejo, J.J., van Vliet, S.J., and van Kooyk, Y. (2014). DCIR interacts with ligands from both endogenous and pathogenic origin. Immunol. Lett. *158*, 33–41.

Boubou, M.I., Collette, A., Voegtlé, D., Mazier, D., Cazenave, P.A., and Pied, S. (1999). T cell response in malaria pathogenesis: selective increase in T cells carrying the TCR V(beta)8 during experimental cerebral malaria. Int. Immunol. *11*, 1553–1562.

Cambos, M., Bazinet, S., Abed, E., Sanchez-Dardon, J., Bernard, C., Moreau, R., Olivier, M., and Scorza, T. (2010). The IL-12p70/IL-10 interplay is differentially regulated by free heme and hemozoin in murine bone-marrow-derived macrophages. Int. J. Parasitol. *40*, 1003–1012.

Coban, C., Ishii, K.J., Kawai, T., Hemmi, H., Sato, S., Uematsu, S., Yamamoto, M., Takeuchi, O., Itagaki, S., Kumar, N., et al. (2005). Toll-like receptor 9 mediates innate immune activation by the malaria pigment hemozoin. J. Exp. Med. *201*, 19–25.

Coban, C., Ishii, K.J., Uematsu, S., Arisue, N., Sato, S., Yamamoto, M., Kawai, T., Takeuchi, O., Hisaeda, H., Horii, T., and Akira, S. (2007). Pathological role of Toll-like receptor signaling in cerebral malaria. Int. Immunol. *19*, 67–79.

Coronado, L.M., Nadovich, C.T., and Spadafora, C. (2014). Malarial hemozoin: from target to tool. Biochim. Biophys. Acta *1840*, 2032–2041.

de Oca, M.M., Engwerda, C., and Haque, A. (2013). *Plasmodium berghei* ANKA (PbA) infection of C57BL/6J mice: a model of severe malaria. Methods Mol. Biol. *1031*, 203–213.

deWalick, S., Amante, F.H., McSweeney, K.A., Randall, L.M., Stanley, A.C., Haque, A., Kuns, R.D., MacDonald, K.P., Hill, G.R., and Engwerda, C.R. (2007). Cutting edge: conventional dendritic cells are the critical APC required for the induction of experimental cerebral malaria. J. Immunol. *178*, 6033–6037.

Dostert, C., Guarda, G., Romero, J.F., Menu, P., Gross, O., Tardivel, A., Suva, M.L., Stehle, J.C., Kopf, M., Stamenkovic, I., et al. (2009). Malarial hemozoin is a Nalp3 inflammasome activating danger signal. PLoS ONE *4*, e6510.

Franchina, D.G., Dostert, C., and Brenner, D. (2018). Reactive Oxygen Species: Involvement in T Cell Signaling and Metabolism. Trends Immunol. *39*, 489–502.

Grau, G.E., Piguet, P.F., Engers, H.D., Louis, J.A., Vassalli, P., and Lambert, P.H. (1986). L3T4$^+$ T lymphocytes play a major role in the pathogenesis of murine cerebral malaria. J. Immunol. *137*, 2348–2354.

Haque, A., Best, S.E., Unosson, K., Amante, F.H., de Labastida, F., Anstey, N.M., Karupiah, G., Smyth, M.J., Heath, W.R., and Engwerda, C.R. (2011). Granzyme B expression by CD8$^+$ T cells is required for the development of experimental cerebral malaria. J. Immunol. *186*, 6148–6156.

Hermsen, C., van de Wiel, T., Mommers, E., Sauerwein, R., and Eling, W. (1997). Depletion of CD4$^+$ or CD8$^+$ T-cells prevents *Plasmodium berghei* induced cerebral malaria in end-stage disease. Parasitology *114*, 7–12.

Hermsen, C.C., Mommers, E., van de Wiel, T., Sauerwein, R.W., and Eling, W.M. (1998). Convulsions due to increased permeability of the blood-brain barrier in experimental cerebral malaria can be prevented by splenectomy or anti-T cell treatment. J. Infect. Dis. *178*, 1225–1227.

Hutten, T.J., Thordardottir, S., Fredrix, H., Janssen, L., Woestenenk, R., Tel, J., Joosten, B., Cambi, A., Heemskerk, M.H., Franssen, G.M., et al. (2016). CLEC12A-mediated antigen uptake and cross-presentation by human dendritic cell subsets efficiently boost tumor-reactive T cell responses. J. Immunol. *197*, 2715–2725.

Janas, M.L., Groves, P., Kienzle, N., and Kelso, A. (2005). IL-2 regulates perforin and granzyme gene expression in CD8$^+$ T cells independently of its effects on survival and proliferation. J. Immunol. *175*, 8003–8010.

Jaramillo, M., Bellemare, M.J., Martel, C., Shio, M.T., Contreras, A.P., Godbout, M., Roger, M., Gaudreault, E., Gosselin, J., Bohle, D.S., and Olivier, M. (2009). Synthetic *Plasmodium*-like hemozoin activates the immune response: a morphology - function study. PLoS ONE *4*, e6957.

Krishnegowda, G., Hajjar, A.M., Zhu, J., Douglass, E.J., Uematsu, S., Akira, S., Woods, A.S., and Gowda, D.C. (2005). Induction of proinflammatory responses in macrophages by the glycosylphosphatidylinositols of *Plasmodium falciparum*: cell signaling receptors, glycosylphosphatidylinositol (GPI) structural requirement, and regulation of GPI activity. J. Biol. Chem. *280*, 8606–8616.

Lahoud, M.H., Proietto, A.I., Ahmet, F., Kitsoulis, S., Eidsmo, L., Wu, L., Sathe, P., Pietersz, S., Chang, H.W., Walker, I.D., et al. (2009). The C-type lectin Clec12A present on mouse and human dendritic cells can serve as a target for antigen delivery and enhancement of antibody responses. J. Immunol. *182*, 7587–7594.

Lambros, C., and Vanderberg, J.P. (1979). Synchronization of *Plasmodium falciparum* erythrocytic stages in culture. J. Parasitol. *65*, 418–420.

Lepenies, B., Pfeffer, K., Hurchla, M.A., Murphy, T.L., Murphy, K.M., Oetzel, J., Fleischer, B., and Jacobs, T. (2007). Ligation of B and T lymphocyte attenuator prevents the genesis of experimental cerebral malaria. J. Immunol. *179*, 4093–4100.

Lepenies, B., Cramer, J.P., Burchard, G.D., Wagner, H., Kirschning, C.J., and Jacobs, T. (2008). Induction of experimental cerebral malaria is independent of TLR2/4/9. Med. Microbiol. Immunol. (Berl.) *197*, 39–44.

Lundie, R.J., de Koning-Ward, T.F., Davey, G.M., Nie, C.Q., Hansen, D.S., Lau, L.S., Mintern, J.D., Belz, G.T., Schofield, L., Carbone, F.R., et al. (2008). Blood-stage *Plasmodium* infection induces CD8$^+$ T lymphocytes to parasite-expressed antigens, largely regulated by CD8α^+ dendritic cells. Proc. Natl. Acad. Sci. USA *105*, 14509–14514.

Maglinao, M., Klopfleisch, R., Seeberger, P.H., and Lepenies, B. (2013). The C-type lectin receptor DCIR is crucial for the development of experimental cerebral malaria. J. Immunol. *191*, 2551–2559.

Maglinao, M., Eriksson, M., Schlegel, M.K., Zimmermann, S., Johannssen, T., Götze, S., Seeberger, P.H., and Lepenies, B. (2014). A platform to screen for C-type lectin receptor-binding carbohydrates and their potential for cell-specific targeting and immune modulation. J. Control. Release *175*, 36–42.

Monteiro, J.T., Schön, K., Ebbecke, T., Goethe, R., Ruland, J., Baumgärtner, W., Becker, S.C., and Lepenies, B. (2019). The CARD9-associated C-type lectin, Mincle, recognizes La Crosse Virus (LACV) but plays a limited role in early antiviral responses against LACV. Viruses *11*, E303.

Moro-García, M.A., Mayo, J.C., Sainz, R.M., and Alonso-Arias, R. (2018). Influence of inflammation in the process of T lymphocyte differentiation: proliferative, metabolic, and oxidative changes. Front. Immunol. *9*, 339.

Neumann, K., Castiñeiras-Vilariño, M., Höckendorf, U., Hannesschläger, N., Lemeer, S., Kupka, D., Meyermann, S., Lech, M., Anders, H.J., Kuster, B., et al. (2014). Clec12a is an inhibitory receptor for uric acid crystals that regulates inflammation in response to cell death. Immunity *40*, 389–399.

Newton, C.R., Taylor, T.E., and Whitten, R.O. (1998). Pathophysiology of fatal falciparum malaria in African children. Am. J. Trop. Med. Hyg. *58*, 673–683.

Nguyen, P.H., Day, N., Pram, T.D., Ferguson, D.J., and White, N.J. (1995). Intraleucocytic malaria pigment and prognosis in severe malaria. Trans. R. Soc. Trop. Med. Hyg. *89*, 200–204.

Nitcheu, J., Bonduelle, O., Combadiere, C., Tefit, M., Seilhean, D., Mazier, D., and Combadiere, B. (2003). Perforin-dependent brain-infiltrating cytotoxic

CD8$^+$ T lymphocytes mediate experimental cerebral malaria pathogenesis. J. Immunol. *170*, 2221–2228.

Oberkampf, M., Guillerey, C., Mouriès, J., Rosenbaum, P., Fayolle, C., Bobard, A., Savina, A., Ogier-Denis, E., Enninga, J., Amigorena, S., et al. (2018). Mitochondrial reactive oxygen species regulate the induction of CD8$^+$ T cells by plasmacytoid dendritic cells. Nat. Commun. *9*, 2241.

Olivier, M., Van Den Ham, K., Shio, M.T., Kassa, F.A., and Fougeray, S. (2014). Malarial pigment hemozoin and the innate inflammatory response. Front. Immunol. *5*, 25.

Parroche, P., Lauw, F.N., Goutagny, N., Latz, E., Monks, B.G., Visintin, A., Halmen, K.A., Lamphier, M., Olivier, M., Bartholomeu, D.C., et al. (2007). Malaria hemozoin is immunologically inert but radically enhances innate responses by presenting malaria DNA to Toll-like receptor 9. Proc. Natl. Acad. Sci. USA *104*, 1919–1924.

Piva, L., Tetlak, P., Claser, C., Karjalainen, K., Renia, L., and Ruedl, C. (2012). Cutting edge: Clec9A$^+$ dendritic cells mediate the development of experimental cerebral malaria. J. Immunol. *189*, 1128–1132.

Potter, S., Chan-Ling, T., Ball, H.J., Mansour, H., Mitchell, A., Maluish, L., and Hunt, N.H. (2006). Perforin mediated apoptosis of cerebral microvascular endothelial cells during experimental cerebral malaria. Int. J. Parasitol. *36*, 485–496.

Pyz, E., Huysamen, C., Marshall, A.S., Gordon, S., Taylor, P.R., and Brown, G.D. (2008). Characterisation of murine MICL (CLEC12A) and evidence for an endogenous ligand. Eur. J. Immunol. *38*, 1157–1163.

Sagar, D., Singh, N.P., Ginwala, R., Huang, X., Philip, R., Nagarkatti, M., Nagarkatti, P., Neumann, K., Ruland, J., Andrews, A.M., et al. (2017). Antibody blockade of CLEC12A delays EAE onset and attenuates disease severity by impairing myeloid cell CNS infiltration and restoring positive immunity. Sci. Rep. *7*, 2707.

Schwarzer, E., and Arese, P. (1996). Phagocytosis of malarial pigment hemozoin inhibits NADPH-oxidase activity in human monocyte-derived macrophages. Biochim. Biophys. Acta *1316*, 169–175.

Scorza, T., Magez, S., Brys, L., and De Baetselier, P. (1999). Hemozoin is a key factor in the induction of malaria-associated immunosuppression. Parasite Immunol. *21*, 545–554.

Shio, M.T., Eisenbarth, S.C., Savaria, M., Vinet, A.F., Bellemare, M.J., Harder, K.W., Sutterwala, F.S., Bohle, D.S., Descoteaux, A., Flavell, R.A., and Olivier, M. (2009). Malarial hemozoin activates the NLRP3 inflammasome through Lyn and Syk kinases. PLoS Pathog. *5*, e1000559.

Shio, M.T., Kassa, F.A., Bellemare, M.J., and Olivier, M. (2010). Innate inflammatory response to the malarial pigment hemozoin. Microbes Infect. *12*, 889–899.

Sullivan, A.D., Ittarat, I., and Meshnick, S.R. (1996). Patterns of haemozoin accumulation in tissue. Parasitology *112*, 285–294.

Tamang, D.L., Redelman, D., Alves, B.N., Vollger, L., Bethley, C., and Hudig, D. (2006). Induction of granzyme B and T cell cytotoxic capacity by IL-2 or IL-15 without antigens: multiclonal responses that are extremely lytic if triggered and short-lived after cytokine withdrawal. Cytokine *36*, 148–159.

Togbe, D., Schofield, L., Grau, G.E., Schnyder, B., Boissay, V., Charron, S., Rose, S., Beutler, B., Quesniaux, V.F., and Ryffel, B. (2007). Murine cerebral malaria development is independent of toll-like receptor signaling. Am. J. Pathol. *170*, 1640–1648.

Trang, D.T., Huy, N.T., Kariu, T., Tajima, K., and Kamei, K. (2004). One-step concentration of malarial parasite-infected red blood cells and removal of contaminating white blood cells. Malar. J. *3*, 7.

Tyberghein, A., Deroost, K., Schwarzer, E., Arese, P., and Van den Steen, P.E. (2014). Immunopathological effects of malaria pigment or hemozoin and other crystals. Biofactors *40*, 59–78.

Wakim, L.M., Smith, J., Caminschi, I., Lahoud, M.H., and Villadangos, J.A. (2015). Antibody-targeted vaccination to lung dendritic cells generates tissue-resident memory CD8 T cells that are highly protective against influenza virus infection. Mucosal Immunol. *8*, 1060–1071.

WHO (2017). World Malaria Report 2017. https://www.who.int/malaria/publications/world-malaria-report-2017/report/en/.

Yañez, D.M., Manning, D.D., Cooley, A.J., Weidanz, W.P., and van der Heyde, H.C. (1996). Participation of lymphocyte subpopulations in the pathogenesis of experimental murine cerebral malaria. J. Immunol. *157*, 1620–1624.

STAR★METHODS

KEY RESOURCES TABLE

REAGENT or RESOURCE	SOURCE	IDENTIFIER
Antibodies		
Goat anti-human IgG (Fc) AP	Jackson ImmunoResearch Labs	CAT#109-055-008; RRID:AB_2337601
Goat anti-human IgG (Fc) PE	Jackson ImmunoResearch Labs	CAT#109-115-098; RRID:AB_2337675
Goat anti-human IgG (Fc) Alexa Fluor 488	Jackson ImmunoResearch Labs	CAT#109-545-098; RRID:AB_2337840
Rat anti-mouse CD16/32	eBioscience (Thermo Fisher Scientific)	CAT#14-0161-86; RRID:AB_467135
Rat anti-mouse CD4 APC-eFluor®780	eBioscience (Thermo Fisher Scientific)	CAT#47-0042-82; RRID:AB_1272183
Armenian hamster anti-mouse CD11c APC	eBioscience (Thermo Fisher Scientific)	CAT#17-0114-82; RRID:AB_469346
Mouse anti-mouse MHC-II FITC	eBioscience (Thermo Fisher Scientific)	CAT#11-5320-82; RRID:AB_2572501
Rat anti-mouse CD86 PE	eBioscience (Thermo Fisher Scientific)	CAT#12-0862-83; RRID:AB_465769
Rat anti-mouse CD4 FITC	eBioscience (Thermo Fisher Scientific)	CAT#11-0041-85; RRID:AB_464893
Rat anti-mouse CD8a PE	BD Bioscience	CAT#561095; RRID:AB_2034011
Rat anti-mouse CD62L PE-Cy7	eBioscience (Thermo Fisher Scientific)	CAT#25-0621-82; RRID:AB_469633
Armenian hamster anti-mouse CD69 APC	eBioscience (Thermo Fisher Scientific)	CAT#17-0691-82; RRID:AB_1210795
Rat anti-mouse CD8a FITC	eBioscience (Thermo Fisher Scientific)	CAT#11-0081-82; RRID:AB_464915
Rat anti-mouse Granzyme B APC	eBioscience (Thermo Fisher Scientific)	CAT#17-8898-82; RRID:AB_2688068
Rat anti-mouse IL-2 APC	eBioscience (Thermo Fisher Scientific)	CAT#17-7021-82; RRID:AB_469490
Rat anti-mouse TNF-α APC	eBioscience (Thermo Fisher Scientific)	CAT#17-7321-82; RRID:AB_469508
Rat anti-mouse IFN-γ APC	BD Bioscience	CAT#554413; RRID:AB_398551
Rat anti-mouse CLEC12A PE	BioLegend	CAT#143403; RRID:AB_11126747
Rat anti-mouse CD4 FITC	Miltenyi Biotec	CAT#130-091-608; RRID:AB_244286
Rat anti-mouse CD8a APC	Miltenyi Biotec	CAT#130-091-606; RRID:AB_244291
Hamster anti-mouse CD69 PerCP-Cy5.5	eBioscience (Thermo Fisher Scientific)	CAT#45-0691-82; RRID:AB_1210703
Rat anti-mouse CD8 APC-H7	BD Bioscience	CAT#560182; RRID:AB_1645237
Rat anti-mouse CD45 PerCP	Miltenyi Biotec	CAT#130-094-962; RRID:AB_10828455
Rat anti-mouse CD62L PE	Miltenyi Biotec	CAT#130-091-794; RRID:AB_244290
Chemicals, Peptides, and Recombinant Proteins		
C-type lectin receptor Fc fusion proteins	Maglinao et al., 2014; Monteiro et al., 2019; Neumann et al., 2014	N/A
pFuse-hIgG1-Fc	InvivoGen	CAT#pfuse-hg1fc2
Freestyle CHO Expression medium	Fisher Scientific	CAT#10546183
Freestyle MAX reagent	Fisher Scientific	CAT#10259172
Hemozoin	Invivogen	CAT#tlrl-hz
7-AAD viability staining solution	eBioscience (Thermo Fisher Scientific)	CAT#00-6993-50
Phorbol-12-myristate-13-acetate (PMA)	AppliChem	CAT#A0903,0001
Dihydrorhodamine (DHR)-123	Sigma-Aldrich	CAT#D1054-2MG
OVA-AlexaFluor 488	Thermo Fisher Scientific	CAT#O34781
DQ™ OVA	Thermo Fisher Scientific	CAT#D12053
LPS	Sigma-Aldrich	CAT#L4391-1MG
EndoGrade® ovalbumin	Hyglos	CAT#321001
GolgiPlug	BD Biosciences	CAT#555029
Ionomycin	Sigma-Aldrich	CAT#I0634-1MG
Critical Commercial Assays		
Murine TNF-α Standard ABTS ELISA Development Kit	PeproTech	CAT#900-K54

(*Continued on next page*)

Continued

REAGENT or RESOURCE	SOURCE	IDENTIFIER
Murine IL-12 Standard ABTS ELISA Development Kit	PeproTech	CAT#900-K97
Murine IL-2 Standard ABTS ELISA Development Kit	PeproTech	CAT#900-K108
Murine IFN-γ Standard ABTS ELISA Development Kit	PeproTech	CAT#900-K98
Granzyme B Mouse Uncoated ELISA Kit	Thermo Fisher Scientific	CAT#88-8022-88; RRID: AB_2575171
Pan T Cell Isolation Kit II mouse	Miltenyi Biotec	CAT# 130-095-130
Experimental Models: Cell Lines		
mCLEC12A, hCLEC12A, mCLEC7A A5 T cell hybridoma reporter cell lines	Neumann et al., 2014	N/A
Experimental Models: Organisms/Strains		
CLEC12A$^{-/-}$ mice	Neumann et al., 2014	N/A
OT-I C57BL/6-Tg(TcraTcrb)1100Mjb/Crl mice	Charles River	CAT#642OT1
OT-II C57BL/6-Tg(TcraTcrb)425Cbn/J mice	own breeding	N/A
Oligonucleotides		
Primer for CLEC12A genotyping: WT-Fw: 5′-CTGTATGCCCTTAATACACCTCCTGC-3′	Neumann et al., 2014	N/A
KO-Fw: 5'-GGTGGGATTAGATAAATGCCTGC-3′	Neumann et al., 2014	N/A
Rv: 5'-CCATGAACAATGAGGAGAGAAGCC-3′	Neumann et al., 2014	N/A
Software and Algorithms		
GraphPad Prism Version 7	GraphPad Software	N/A
FlowJo Version 10	FlowJo LLC	N/A

LEAD CONTACT AND MATERIALS AVAILABILITY

Further information and request for resources and reagents should be directed to and will be fulfilled by the Lead Contact, Bernd Lepenies (Bernd.Lepenies@tiho-hannover.de).

EXPERIMENTAL MODEL AND SUBJECT DETAILS

Mouse model

The generation of CLEC12A$^{-/-}$ mice was described previously and mice were backcrossed to C57BL/6 background for ten generations (Neumann et al., 2014). The genotype of the CLEC12A$^{-/-}$ mice was confirmed by PCR (WT-Fw: 5′-CTGTATGCCCTTAAT ACACCTCCTGC-3′; KO-Fw: 5'-GGTGGGATTAGATAAATGCCTGC-3′; Rv: 5'-CCATGAACAATGAGGAGAGAAGCC-3′) and flow cytometric analysis of spleen and bone marrow cells using PE-conjugated anti-mouse CLEC12A antibody (5D3/CLEC12A, BioLegend, San Diego, CA, 1:200). Mice were kept and bred in the animal facility of the Federal Institute for Risk Assessment (Berlin, Germany) under specific pathogen-free conditions and provided food and water *ad libitum*. Female CLEC12A$^{-/-}$ mice or the respective C57BL/6 wild-type control mice were used for PbA infection experiments at 6-10 weeks of age and maintained on a 12:12 hr light-dark cycle. Experiments were permitted by the Ethics Commission of the Institutional Animal Care and Use Committee (IACUC) of the Regional Office for Health and Social Affairs Berlin under reference numbers G0053/10 and G0198/14 and/or the German Lower Saxony State Office for Consumer Protection and Food Safety under reference number 33.12-42502-04-15/1936. All efforts were made to minimize suffering. Sacrificing of mice for scientific purposes was approved by the Animal Welfare Officers of the University of Veterinary Medicine Hannover (AZ 02.05.2016).

Primary cell culture

Bone marrow cells were obtained from femur and tibia of CLEC12A$^{-/-}$ and C57BL/6 control mice (own breeding) and were differentiated into BMDCs using differentiation medium (IMDM medium, 10% fetal bovine serum, 2 mM L-glutamine, 100 U/ml penicillin 100 μg/ml streptomycin, 10% X63-GM-CSF supernatant) at 37°C and 5% CO_2 for 8 to 10 days. Mice used for bone marrow extraction were not restricted to a specific age or gender. They were maintained under specific pathogen-free conditions on a 12:12 hr light-dark cycle in the animal facility of the Institute for Physiological Chemistry of the University of Veterinary Medicine Hannover, Foundation.

METHOD DETAILS

Culture of *Plasmodium* species

The *Plasmodium falciparum* 3D7 line was cultured in human erythrocytes (0+) from healthy donors. Cultures were maintained at a hematocrit of 2.7% in 3D7 culture medium (RPMI 1640, 0.5% Albumax II, 5 mM HEPES, 2 mM L-glutamine, 28 μg/ml hypoxanthine, 50 μg/ml gentamicin). Cultures were incubated in an anaerobic jar flushed with a gas mixture of 95% N_2, 5% CO_2, and 2% O_2 at 37°C. Medium was replaced daily and parasitemia was estimated by Giemsa staining of thin blood smears. Parasitemia was routinely kept at 1%–10%. Cultures were synchronized by incubating parasites every 96 hours with 5% D-sorbitol for 10min (Lambros and Vanderberg, 1979).

The PbA strains 1008M and MRA-311 were kindly provided by PD Dr. Thomas Jacobs (Bernhard Nocht Institute for Tropical Medicine, Hamburg, Germany). Stabilates were prepared by passage through BALB/c mice. Parasitized RBCs were snap frozen in 0.9% NaCl, 4.2% D-sorbitol, and 28% glycerol and used for subsequent infection experiments.

CLR-hFc binding assays

Lysates of *Plasmodium*-infected RBCs were derived from synchronized late-stage parasites by magnetic activated cell sorting. Blood obtained from PbA-infected BALB/c mice was diluted in PBS and loaded onto an LD column (Miltenyi Biotec, Bergisch Gladbach, Germany). The column was washed with MACS buffer (PBS, 1% BSA, 2mM EDTA), followed by elution of infected cells (Trang et al., 2004). Purity of late-stage parasites was confirmed by Giemsa staining of thin blood smears and RBCs were subsequently lysed with ultrapure water.

The generation of the CLR-hFc fusion protein library was described previously (Maglinao et al., 2014; Monteiro et al., 2019). Sequences encoding the extracellular domain of indicated CLRs were ligated into the expression vector pFuse-hIgG1-Fc (InvivoGen, San Diego, CA). Constructs were subsequently used to transiently transfect CHO-S cells using the FreeStyle Max CHO-S Expression System (Life Technologies, Darmstadt, Germany) or for generation of stable CLR-hFc expressing CHO cells. Soluble fusion proteins were purified from the supernatant by affinity chromatography using protein G columns (GE Healthcare, Little Chalfont, UK). Purity and identity were confirmed by SDS-PAGE and hFc-specific western blot, respectively.

For ELISA-based binding assays, lysates of *Plasmodium*-infected RBCs were coated on high-binding 96-well microtiter ELISA plates (Greiner Bio-One, Kremsmünster, Austria) at RT overnight, corresponding to 2.5×10^5 pRBCs per well. The next day, wells were blocked using 1% BSA in PBS for 2h at RT, followed by the addition of CLR-hFc fusion proteins at 5 μg/ml in lectin buffer/BSA (50 mM HEPES, 0.5% BSA, 5 mM $CaCl_2$, 5 mM $MgCl_2$, pH 7.4) for 2h at RT. Binding was detected after incubation with AP-conjugated anti-human IgG (Fc) antibody (MinX, Jackson ImmunoResearch Labs, Cambridgeshire, UK) 1:5000 in reagent diluent (1% BSA, 0.05% Tween 20 in PBS) and colorimetric detection using pNPP as substrate. After each step, plates were washed with 0.05% Tween 20® in PBS.

Synthetic hemozoin (InvivoGen) was incubated for 2h at 4°C with indicated hFc-fusion proteins in DMEM containing 10% FBS, washed with PBS 1% FBS and bound hFc-fusion proteins were stained with anti-human IgG (Fc)-PE (MinX, Jackson ImmunoResearch Labs) 1:100 in 0.5% PBS/BSA for 30min at 4°C. PE fluorescence of hemozoin particles was analyzed by flow cytometry. To confirm CLEC12A-hFc binding to hemozoin in the presence of higher protein concentrations, selected experiments were also performed DMEM containing 20% FBS and 50% FBS, respectively (data not shown).

Fluorescence microscopy

PbA-infected RBCs were fixed in 1% PFA for 10min at RT with subsequent permeabilization with 0.1% saponin in lectin binding buffer (50 mM HEPES, 1% BSA, 5 mM $CaCl_2$, 5 mM $MgCl_2$, pH 7.4) for 10min at RT. RBCs were stained with the indicated fusion proteins at 5μg/ml in saponin-supplemented lectin binding buffer for 2h at 4°C followed by incubation with an anti-human IgG (Fc) Alexa Fluor 488-labeled antibody (Jackson ImmunoResearch Labs) in saponin-supplemented 1% FBS in PBS (1:200 dilution) for 1h at 4°C. Stained samples were applied to poly-L-lysine-coated cover slides for 90min at 37°C and mounted into proLong™ Gold antifade mountant containing DAPI (Invitrogen). Fluorescence was detected using a TCS SP5 confocal inverted-base fluorescence microscope (Leica, Nussloch, Germany).

Synthetic hemozoin (InvivoGen) was incubated with the indicated hFc-fusion proteins at 10 μg/ml in DMEM 10% FBS for 2h at 4°C. Binding was detected using an anti-human IgG (Fc) Alexa Fluor 488-labeled antibody (Jackson ImmunoResearch Labs) diluted 1:200 in 1% FBS in PBS for 2h at 4°C. Samples were applied to microscopic slides and mounted into Eukitt® quick hardening mounting medium (Sigma-Aldrich, St. Louis, MO). Fluorescence was detected using an Axio Imager M2 microscope (Zeiss, Oberkochen, Germany).

Scanning electron microscopy

Crystals were applied to 12,7 mm SEM stubs (Science Services, München, Germany) and gold sputtered using a Q150R-S sputter coater (Quorum Technologies, Laughton, UK) for 240 s at a sputter current of 20 mA and a tooling factor set to 2.30. Samples were transferred directly to a Crossbeam 540 KMAT SEM (Zeiss, Oberkochen, Germany) equipped with a thermic Schottky-emitter, using a sample lock. Imaging was done at 10 kV acceleration voltage at a magnification of 15.000x and a chamber vacuum of 3×10^{-6} mBar, using a Everhart-Thornley chamber secondary electron detector. Scan speed was set to step 11, probe current was 500 pA.

Reporter cell line assay

A5 T cell hybridoma reporter cell lines expressing murine CLEC7A, murine CLEC12A and human CLEC12A, respectively (Neumann et al., 2014), were cultured in selection medium (RPMI 1640, 5% FBS, 2 mM L-glutamine, 1 mg/ml G418) at 37°C and 5% CO_2. On day 4, reporter cells were transferred to assay medium (RPMI 1640, 0.5% FBS, 2 mM L-glutamine). Cells were seeded in a 96-well plate at a concentration of 8 × 10^5 cells/ml and stimulated with MSU (250 μg/ml), hemozoin (100 μg/ml, InvivoGen), lysates of parasitized RBCs (ratio 20:1) and lysates of uninfected RBCs (ratio 20:1) at 37°C and 5% CO_2 for 18h. Afterward, cells were blocked with anti-mouse CD16/32 (93, eBioscience, Frankfurt am Main, Germany, 1:100) for 10min at 4°C and stained with anti-mouse CD4 APC-eFluor®780 (RM4-5, eBioscience, 1:200) as a reporter cell staining for 20min at 4°C. 7-AAD (eBioscience, 1:80) was used as a viability staining for 15min at RT. GFP expression of stained cells was analyzed by an Attune NxT Flow Cytometer (Thermo Fisher Scientific, Waltham, MA). Data analysis was performed using FlowJo (Version 10, FlowJo LLC., Ashland, OR).

ROS assay

Bone marrow cells were obtained from femur and tibia of CLEC12A$^{-/-}$ and C57BL/6 control mice (own breeding) and were differentiated into BMDCs using differentiation medium (IMDM medium, 10% fetal bovine serum, 2 mM L-glutamine, 100 U/ml penicillin 100 μg/ml streptomycin, 10% X63-GM-CSF supernatant) at 37°C and 5% CO_2. After 8 to 10 days of differentiation, BMDCs were seeded at a concentration of 5 × 10^5 cells/ml in a 96-well plate and incubated with hemozoin (100 μg/ml, InvivoGen) at 37°C and 5% CO_2 for 4h or 24h. Cells were stimulated with PMA (100 ng/ml, AppliChem, Darmstadt, Germany) for 15min followed by addition of dihydrorhodamine (DHR)-123 (0.5 μg/ml, Sigma-Aldrich) for 15min at 37°C and 5% CO_2. Cells were blocked with anti-mouse CD16/32 (93, eBioscience, 1:100) for 10min at 4°C and stained with APC-conjugated anti-mouse CD11c (N418, eBioscience, 1:200) for 20min at 4°C. ROS production was analyzed using an Attune NxT Flow Cytometer (Thermo Fisher Scientific).

OVA uptake and processing

Bone marrow cells were differentiated as described above (ROS assay). After 8 to 10 days of differentiation, BMDCs were seeded at a concentration of 5 × 10^5 cells/ml in a 96-well plate and stimulated with OVA-Alexa Fluor 488 (25 μg/ml, Thermo Fisher Scientific) or DQ™ OVA (25 μg/ml, Thermo Fisher Scientific) in the presence or absence of hemozoin (50, 20 μg/ml, InvivoGen) at 37°C and 5% CO_2 for 45min. Subsequently, cells were blocked with anti-mouse CD16/32 (93, eBioscience, 1:100) for 10min at 4°C and stained with APC-conjugated anti-mouse CD11c (N418, eBioscience, 1:200) for 20min at 4°C. Samples were analyzed by an Attune NxT Flow Cytometer (Thermo Fisher Scientific).

DC stimulation assay

Bone marrow cells were differentiated as described above (ROS assay). After 8 to 10 days of differentiation, BMDCs were seeded at a concentration of 5 × 10^5 cells/ml in a 96-well plate and stimulated with LPS (1 ng/ml, Sigma-Aldrich) in the presence or absence of hemozoin (100, 50 μg/ml, InvivoGen) at 37°C and 5% CO_2 for 24h. On the next day, supernatants were harvested and cytokine concentrations were measured by ELISA (Murine TNF-α Standard ABTS ELISA Development Kit, Murine IL-12 Standard ABTS ELISA Development Kit, PeproTech, Hamburg, Germany). BMDCs were blocked with anti-mouse CD16/32 (93, eBioscience, 1:100) for 10min at 4°C and stained with APC-conjugated anti-mouse CD11c (N418, eBioscience, 1:200), FITC-conjugated anti-mouse MHC-II (AF6-120.1, eBioscience, 1:100) and PE-conjugated anti-mouse CD86 (B7-2, eBioscience, 1:200) for 20min at 4°C. Samples were analyzed using an Attune NxT Flow Cytometer (Thermo Fisher Scientific).

DC-T cell co-culture assay

Bone marrow cells were differentiated as described above (ROS assay). After 8 to 10 days of differentiation, BMDCs were seeded at a concentration of 2 × 10^5 cells/ml in a 96-well plate and stimulated with EndoGrade® ovalbumin (0.3 mg/ml, Hyglos, Bernried, Germany) in the presence or absence of hemozoin (100, 50, 20 μg/ml, InvivoGen) at 37°C and 5% CO_2 for 24h. T cells were isolated from spleens of 8 to 14 week old OT-I (purchased from Charles River, Sulzfeld, Germany) and OT-II (own breeding) transgenic mice via magnetic-activated cell sorting (Pan T Cell Isolation Kit II mouse, Miltenyi Biotec). Purified T cells were adjusted to 1 × 10^6 cells/ml and co-cultured with BMDCs at 37°C and 5% CO_2 overnight or for 72h, respectively.

After overnight incubation, intracellular granzyme B, IL-2, TNF-α and IFN-γ levels were determined upon restimulation of T cells with PMA (100 ng/ml, AppliChem)/Ionomycin (1 μg/ml, Sigma-Aldrich) in the presence of GolgiPlug (1 μl/ml, BD Biosciences) at 37°C and 5% CO_2 for 3h. Cells were blocked with anti-mouse CD16/32 (93, eBioscience, 1:100) for 10min at 4°C and stained using FITC-conjugated anti-mouse CD8a (53-6.7, eBioscience, 1:100) for 20min at 4°C followed by fixation with 1% PFA for 20min at RT. Subsequently, cells were permeabilized with saponin buffer (0.5% saponin, 1% FBS in PBS) for 10min at RT and stained for intracellular cytokines with APC-conjugated anti-mouse granzyme B (NGZB, eBioscience), anti-IL-2 (JES6-5H4, eBioscience), anti-TNF-α (MP6-XT22, eBioscience) or anti-IFN-γ (XMG1.2, BD Biosciences, Franklin Lakes, NJ), respectively, diluted 1:200 in permeabilization buffer for 20min at RT. Samples were analyzed using an Attune NxT Flow Cytometer (Thermo Fisher Scientific).

After 72h of incubation, supernatants were harvested and GrB, IL-2, TNF-α and IFN-γ cytokine concentrations were measured by ELISA (Granzyme B Mouse Uncoated ELISA Kit, Thermo Fisher Scientific, Murine IL-2 Standard ABTS ELISA Development Kit, Murine TNF-α Standard ABTS ELISA Development Kit, Murine IFN-γ Standard ABTS ELISA Development Kit, PeproTech). Lymphocytes were blocked with anti-mouse CD16/32 (93, eBioscience, 1:100) for 10min at 4°C and either stained with FITC-conjugated

anti-mouse CD4 (RM4-5, eBioscience, 1:100) or PE-conjugated anti-mouse CD8a (53-6.7, BD Bioscience, 1:200) and PE-Cy7-conjugated anti-mouse CD62L (MEL-14, eBioscience, 1:200) as well as APC-conjugated anti-mouse CD69 (H1.2F3, eBioscience, 1:200) for 20min at 4°C. Samples were analyzed using an Attune NxT Flow Cytometer (Thermo Fisher Scientific).

Challenge of mice with PbA

Female CLEC12A$^{-/-}$ mice or the respective C57BL/6 wild-type control mice were intraperitoneally injected with 1 × 10^6 PbA-infected RBCs (Lepenies et al., 2007; Maglinao et al., 2013). Body weight and clinical score were monitored during the course of infection, accompanied by daily monitoring for early signs of ECM (more often during ECM development between day 7 and day 10 p.i.). Disease scoring was performed as described previously (de Oca et al., 2013). C57BL/6 mice infected with PbA develop general symptoms such as ruffled fur and hunching as well as ECM-specific symptoms including wobbly gait, convulsions, and limb paralysis. Each symptom was assigned a score of 1. Mice were euthanized at an early stage of ECM to minimize suffering (cumulative score of 3-4). For each following day post sacrifice, a score of 5 was assigned. Parasitemia was determined by examining Giemsa-stained thin blood smears obtained from the tail vein. Parasitemia was denoted as the percentage of pRBCs.

Flow cytometric analysis of T cells

Splenocytes and brain-sequestered T cells were analyzed by flow cytometry. Mice infected with PbA were sacrificed on day 6 p.i.. Spleens were dissected and flushed with complete RPMI (RPMI 1640, 10% FCS, 2 mM L-glutamine, 100 U/ml penicillin, 100 μg/ml streptomycin). Collected cells were treated with RBC lysis buffer (144 mM NH_4Cl, 10 mM Tris-HCl, pH 7.2) at RT for 5min. Splenocytes were incubated with anti-mouse CD16/32 (93, eBioscience, 1:100) for 20min at 4°C and stained using anti-mouse CD4 FITC (GK1.5, Miltenyi Biotec, 1:100), anti-mouse CD8a APC (53-6.7, Miltenyi Biotec, 1:100), and anti-mouse CD69 PerCP-Cy5.5 (H1.2F3, eBioscience, 1:100) for 30min at 4°C. Intracellular granzyme B levels were determined after incubation of splenocytes in complete RPMI supplemented with 1 μl/ml GolgiPlug (BD Biosciences) at 37°C and 5% CO_2 for 3h. Cells were incubated with anti-mouse CD16/32 (93, eBioscience, 1:100) for 20min at 4°C and stained using anti-mouse CD4 FITC (GK1.5, Miltenyi Biotec, 1:200) and anti-mouse CD8 APC-H7 (53-6.7, BD Biosciences, 1:200) for 30min at 4°C. To access intracellular GrB, cells were fixed in 2% PFA in PBS for 20min at RT, permeabilized using 0.5% saponin for 10min at RT, and stained with APC-conjugated anti-mouse granzyme B antibody (NGZB, eBioscience, 1:100) for 30min at 4°C.

Brain sequestration of T cells in PbA-infected mice was investigated using brain homogenates. Brains were isolated from PbA infected mice on day 6 p.i. and homogenized in complete RPMI and filtered through a cell strainer (40 μm). After lysis of RBCs, brain homogenates were blocked with anti-mouse CD16/32 (93, eBioscience, 1:100) for 20min at 4°C and stained with anti-mouse CD45 PerCP (30F11, Miltenyi Biotec, 1:50), anti-mouse CD62L PE (MEL14-H2.100, Miltenyi Biotec, 1:50) and anti-mouse CD8 APC-H7 (53-6.7, BD Biosciences, 1:50) for 30min at 4°C. Intracellular GrB levels of brain homogenates were assessed as described above (Maglinao et al., 2013).

QUANTIFICATION AND STATISTICAL ANALYSIS

All statistical analyses were performed using the GraphPad Prism software (Version 7, La Jolla, CA). For PbA infections, Kaplan-Meyer survival curves were analyzed using the log-rank (Mantel-Cox) test. Time courses for disease score, body weight, and parasitemia were compared by two-way ANOVA. All other data was analyzed by unpaired or paired Student's t test. To exclude hemozoin-independent intrinsic effects between WT and CLEC12A$^{-/-}$ DCs (ROS assay, OVA uptake and processing, DC-T cell co-culture assays), data was normalized to the respective positive controls and depicted as fold increase or percentage in relation to control. In Figures 1, 2, 3, and S1–S3, n represents the number of biological replicates. In the PbA infection experiments (Figures 4 and S4), n represents the number of animals. Statistical details, including biological and technical replicates and animal numbers, are provided in the respective figure legends. A *p-value* of $p < 0.05$ was considered statistically significant.